Contrib. Astron. Obs. Skalnaté Pleso **38**, 33 – 46, (2008)

The dynamics of the Oort cloud during a passage through a spherical giant interstellar cloud with the Gaussian-density profile

M. Jakubík and L. Neslušan

Astronomical Institute of the Slovak Academy of Sciences
059 60 Tatranská Lomnica, The Slovak Republic, (E-mail: mjakubik@ta3.sk, ne@ta3.sk)

Received: October 10, 2007; Accepted: January 21, 2008

Abstract. The distant comet reservoir, the Oort cloud, is perturbed by the Galactic tide, nearly passing stars, and giant interstellar molecular clouds. The perturbations by the latter are least frequent, but their amplitude is expected to be highest. In this work, we suggest a simple model of a giant molecular cloud and investigate the gravitational effect of such an object, when the Sun with the Oort cloud goes across it. More specifically, we assume a molecular cloud consisting of a single or two spherical condensations, each with the density profile described by a Gaussian-distribution function. We demonstrate that the final perturbation effect of the molecular cloud on the comet reservoir is quite small. The directional distribution of comet orbits remains almost intact. The outer part of the comet cloud is eroded, but the erosion rate is not fatal for the cloud: we found the maximum rate of 22% of the population. The erosion by the two-condensation molecular cloud is lower than that by a single-condensation molecular cloud, in the studied examples.
Key words: Oort cloud – giant molecular clouds

1. Introduction

Comets are perturbed by several so-called outer perturbers in their distant reservoir, known as the Oort Cloud (OC). Besides the dominant perturbation by the Galactic tide, comet trajectories are influenced by nearly passing alien stars and interstellar matter concentrated into interstellar clouds.

Among the interstellar clouds, giant molecular clouds (GMCs) are the objects which can significantly perturb the comets in the OC. Probably due to poor knowledge of their internal structure, this perturbation has not been often and comprehensively studied, and gravitational effects of the GMCs on the comet orbits remain uncertain. Consequently, the perturbations by the GMCs have used to be ignored in the dynamical studies of the OC.

A few works concerning the GMC perturbation, however, revealed that the role of the GMCs in the OC-comet dynamics can be important. Bierman (1978) found that the outer part of the OC can considerably be depleted due to collisions with interstellar clouds. Napier & Staniucha (1982) and Clube & Napier

(1984) attempted to prove, so far, that the outer region of the OC, beyond $\approx 10\,000$ AU, was completely destroyed when the solar system encountered the GMCs or their substructures. At the same time, a new population of comets were captured from the GMCs (or, alternatively, comets were drawn to the outer region from the inner comet cloud, below $\approx 10\,000$ AU). They estimated the number density of comets in the GMCs to be about $10^{-1}\,\mathrm{AU}^{-3}$. Other authors (e.g. Hut & Tremaine, 1985; Bailey, 1986), however, objected that Napier & Staniucha and Clube & Napier overestimated or underestimated some parameters of a typical encounter of the solar system with a GMC and demonstrated that the effect of GMCs on the OC is not so extreme.

Recently, Mazeeva (2004) considered three examples of GMCs consisting of several (25 and 7) condensations as well as a GMC with a uniform density distribution and demonstrated a large influence of GMCs on the OC-comet dynamics, especially in the case of structured, multi-condensation GMCs.

In this paper, we describe the first results of an intended more comprehensive study of the OC-comet dynamics during the passages of the solar system through a GMC. Specifically, we analyse, here, a passage of a hypothetical OC through a hypothetical GMC with an internal structure approximated (i) by a spherically symmetric distribution of the matter with the radial density profile described by a Gaussian-distribution function and (ii) by a cloud consisting of two such spherical condensations.

2. The structure of a hypothetical spherical GMC

The GMCs are usually identified and their internal structure studied from CO emission contours (e.g. Solomon et al., 1987), being characterized by the total mass and effective radius. The latter is the radius of a hypothetical sphere containing all the mass of a given GMC. In the given context, a spherical distribution of the GMC density, ρ, is assumed and described by the relation

$$\rho(p) = \rho_1 \left(\frac{R_1}{p} \right)^{\alpha}, \tag{1}$$

where p is the cloud-centric distance, R_1 is the maximum radius of the GMC, and ρ_1 is the density at R_1. The standard value of the power-index α is 1. This value is, however, not fixed. Solomon et al. (1987) demonstrated that the density distribution law with $\alpha = 2$ also fits well an observed photometric behavior.

The important feature of the density law (1) derived from the CO-emission photometry is a truncation of the cloud at $p = R_1$, i.e. $\rho = 0$ for $p > R_1$. This discontinuity makes a correct usage of the law in dynamical studies impossible.

An attempt to extrapolate the density law given by (1) beyond R_1 leads either to an extreme increase of the total mass of the GMC or, when artificially reducing R_1, to an extremely centrally concentrated GMC, i.e. a density behavior, which contradicts the photometric observations. This is valid for both $\alpha = 1$ and $\alpha = 2$.

In this work, we approximate the internal structure of a GMC by several spherical condensations overlapping each other at their borders. The density radial distribution of a given condensation is suggested to be described by an error-Gaussian function. In other words, we regard the condensations as fluctuations of the density of interstellar Galactic gas. So, we suggest the density law

$$\rho(p) = \rho_c \exp\left(-\frac{p^2}{2\sigma^2}\right), \tag{2}$$

where ρ_c is the density in the centre of the condensation and σ is its characteristic dispersion.

The mass of the condensation, M_p, inside the sphere of radius p can be calculated as

$$M_p = 4\pi \int_0^p p^2 \rho(p)\, dp = 4\pi\rho_c p^3 \sum_{i=0}^{\infty} \frac{(-1)^i}{(2i+3).i!} \left(\frac{p}{\sqrt{2}\sigma}\right)^{2i}. \tag{3}$$

The density given by relation (2) approaches to zero at the cloud-centric distance $p \to \infty$. As the radius of a given GMC condensation, R_O, we regard such a cloud-centric distance, where the density falls to the value $\approx 10^{-22}\,\mathrm{kg\,m^{-3}}$, which is characteristic for a free interstellar Galactic environment. The mass of the condensation, M_O, is, subsequently, the mass inside the sphere of radius R_O, i.e. $M_O = M_p(R_O)$. The mass M_O practically represents the whole mass of the condensation. One can demonstrate that $M_O > 0.999\, M_p(p \to \infty)$ for all condensations considered in this work or whatever GMC condensations with the reasonable characteristics fitting the observations.

3. The motion of the Sun through a GMC

Let us consider a GMC consisting of n spherical condensations, each having the density profile described by (2). In the rectangular coordinate system with the origin identical to the mass centre of all condensations, the centre of j-th condensation is characterized by vector $\boldsymbol{P}_j = (U_j, V_j, W_j)$ and the position of the Sun by vector $\boldsymbol{R} = (X, Y, Z)$.

We assume that all the condensations creating the considered GMC can be regarded as stable, situated in exactly fixed positions, during a relatively short period of the passage of the solar system throughout their system. If the heliocentric radius vector of the centre of j-th condensation is denoted by $\boldsymbol{p}_j$, then

$$\boldsymbol{p}_j = \boldsymbol{P}_j - \boldsymbol{R}. \tag{4}$$

Denoting $|\boldsymbol{p}_j| = p_j$, the acceleration vector of the Sun can be given as

$$\ddot{\boldsymbol{R}} = -k^2 \sum_{j=1}^{n} \frac{M_{pj}}{p_j^2} \frac{\boldsymbol{R} - \boldsymbol{P}_j}{p_j}, \tag{5}$$

in the mass-centre coordinate system. We denoted the Gauss gravitational constant by k and the mass of j-th condensation within the sphere of radius p_j by M_{pj}.

If we denote the sum in relation (3) by S_j, i.e.

$$S_j = \sum_{i=0}^{\infty} \frac{(-1)^i}{(2i+3).i!} \left(\frac{p_j}{\sqrt{2}\sigma_j} \right)^{2i}, \tag{6}$$

where σ_j is the density dispersion of j-th condensation, then equation (5) can be rewritten as

$$\ddot{\boldsymbol{R}} = -4\pi k^2 \sum_{j=1}^{n} \rho_{cj} S_j \left(\boldsymbol{R} - \boldsymbol{P}_j \right). \tag{7}$$

The symbol ρ_{cj} stands for the central density of j-th condensation.

The integral of energy can be derived after the scalar multiplication of equation (7) with vector $\dot{\boldsymbol{R}}$ and establishing the potential function

$$F_U = -4\pi k^2 \sum_{j=1}^{n} \rho_{cj} S_{Uj}, \tag{8}$$

where

$$S_{Uj} = 2\sigma_j^2 \sum_{i=0}^{\infty} \frac{(-1)^i}{(2i+2)(2i+3)i!} \left(\frac{p_j}{\sqrt{2}\sigma_j} \right)^{2i+2}. \tag{9}$$

After some routine algebraic operations, the result can be obtained in the form

$$\frac{1}{2} \left(\dot{X}^2 + \dot{Y}^2 + \dot{Z}^2 \right) = F_U + C_U. \tag{10}$$

The integration constant C_U represents the total energy of the system, which is conserved. This constant can be used as a test of the correctness of numerical integration of solar motion through the GMCs.

Besides the integral of energy, we can relatively easily derive one more integral, which is related to the momentum conservation. Its general form for j-th condensation is, however, very complicated. So, we here demonstrate the derivation of this integral only for a GMC consisting of two condensations. For $n = 2$, equations (7) can be written as

$$\ddot{X} = -4\pi k^2 \rho_{c1} S_1 (X - U_1) - 4\pi k^2 \rho_{c2} S_2 (X - U_2), \tag{11}$$

$$\ddot{Y} = -4\pi k^2 \rho_{c1} S_1 (Y - V_1) - 4\pi k^2 \rho_{c2} S_2 (Y - V_2), \tag{12}$$

$$\ddot{Z} = -4\pi k^2 \rho_{c1} S_1 (Z - W_1) - 4\pi k^2 \rho_{c2} S_2 (Z - W_2). \tag{13}$$

When we multiply equation (11) by $Y - V_1$, equation (12) by $-(X - U_1)$, and add these equations, we obtain

$$\ddot{X}(Y - V_1) - \ddot{Y}(X - U_1) = -4\pi k^2 \rho_{c2} S_2 \left[(X - U_2)(Y - V_1) - \right. \\ \left. -(Y - V_2)(X - U_1)\right]. \tag{14}$$

Similarly, multiplying equation (12) by $Z - W_1$, equation (13) by $-(Y - V_1)$, and adding them, we obtain

$$\ddot{Y}(Z - W_1) - \ddot{Z}(Y - V_1) = -4\pi k^2 \rho_{c2} S_2 \left[(Y - V_2)(Z - W_1) - \right. \\ \left. -(Z - W_2)(Y - V_1)\right]. \tag{15}$$

Now, multiplying equation (14) by $(Y - V_2)(Z - W_1) - (Z - W_2)(Y - V_1)$, equation (15) by $(Y - V_2)(X - U_1) - (X - U_2)(Y - V_1)$, and adding these two equations provides

$$\left[\ddot{X}(Y - V_1) - \ddot{Y}(X - U_1)\right] \left[(Y - V_2)(Z - W_1) - (Z - W_2)(Y - V_1)\right] = \\ = \left[\ddot{Y}(Z - W_1) - \ddot{Z}(Y - V_1)\right] \left[(X - U_2)(Y - V_1) - (Y - V_2)(X - U_1)\right]. \tag{16}$$

In further steps, we derive the analogous equations eliminating, in the first step, the second terms on the right-hand sides of equations (11), (12), and (13). So, let us multiply equation (11) by $Y - V_2$, equation (12) by $-(X - U_2)$, and add the two. The resultant equation is

$$\ddot{X}(Y - V_2) - \ddot{Y}(X - U_2) = -4\pi k^2 \rho_{c1} S_1 \left[(X - U_1)(Y - V_2) - \right. \\ \left. -(Y - V_1)(X - U_2)\right]. \tag{17}$$

When equation (12) is multiplied by $Z - W_2$, equation (13) by $-(Y - V_2)$, and these equations are added, then

$$\ddot{Y}(Z - W_2) - \ddot{Z}(Y - V_2) = -4\pi k^2 \rho_{c1} S_1 \left[(Y - V_1)(Z - W_2) - \right. \\ \left. -(Z - W_1)(Y - V_2)\right]. \tag{18}$$

Equation (17) can now be multiplied by $(Y - V_1)(Z - W_2) - (Z - W_1)(Y - V_2)$, equation (15) by $(Y - V_1)(X - U_2) - (X - U_1)(Y - V_2)$, and the last two equations can be added yielding

$$\left[\ddot{X}(Y - V_2) - \ddot{Y}(X - U_2)\right] \left[(Y - V_1)(Z - W_2) - (Z - W_1)(Y - V_2)\right] = \\ = \left[\ddot{Y}(Z - W_2) - \ddot{Z}(Y - V_2)\right] \left[(X - U_1)(Y - V_2) - (Y - V_1)(X - U_2)\right]. \tag{19}$$

Equations (16) and (19) can be handled to

$$\left[\ddot{X}(Y - V_1) - \ddot{Y}(X - U_1)\right] \left[(W_2 - W_1)Y + (V_1 - V_2)Z + \right. \\ \left. + (V_2 W_1 - V_1 W_2)\right] = \left[\ddot{Y}(Z - W_1) - \ddot{Z}(Y - V_1)\right] \\ \left[(V_2 - V_1)X + (U_1 - U_2)Y + (U_2 V_1 - U_1 V_2)\right], \tag{20}$$

$$\left[\ddot{X}(Y-V_2)-\ddot{Y}(X-U_2)\right]\left[(W_1-W_2)Y+(V_2-V_1)Z+\right.$$
$$\left.+(V_1W_2-V_2W_1)\right]=\left[\ddot{Y}(Z-W_2)-\ddot{Z}(Y-V_2)\right]$$
$$\left[(V_1-V_2)X+(U_2-U_1)Y+(U_1V_2-U_2V_1)\right]. \qquad (21)$$

The terms in the second brackets on both left- and right-hand sides are, apart from the sign, equal. After dividing equation (20) by equation (21), the corresponding terms eliminate each other and we obtain

$$\frac{\ddot{X}(Y-V_1)-\ddot{Y}(X-U_1)}{\ddot{X}(Y-V_2)-\ddot{Y}(X-U_2)}=\frac{\ddot{Y}(Z-W_1)-\ddot{Z}(Y-V_1)}{\ddot{Y}(Z-W_2)-\ddot{Z}(Y-V_2)}. \qquad (22)$$

This equation can be arranged to became

$$(W_1-W_2)(\ddot{X}Y-\ddot{Y}X)+(U_1-U_2)(\ddot{Y}Z-\ddot{Z}Y)+$$
$$+(V_1-V_2)(\ddot{Z}X-\ddot{X}Z)+(V_1W_2-V_2W_1)\ddot{X}+$$
$$+(W_1U_2-W_2U_1)\ddot{Y}+(U_1V_2-U_2V_1)\ddot{Z}=0, \qquad (23)$$

which can easily be integrated by time. The resultant integral is

$$(W_1-W_2)(\dot{X}Y-\dot{Y}X)+(U_1-U_2)(\dot{Y}Z-\dot{Z}Y)+$$
$$+(V_1-V_2)(\dot{Z}X-\dot{X}Z)+(V_1W_2-V_2W_1)\dot{X}+$$
$$+(W_1U_2-W_2U_1)\dot{Y}+(U_1V_2-U_2V_1)\dot{Z}=C_m, \qquad (24)$$

where C_m is an integration constant. This invariant can again be used to test the correctness of a numerical integration of the solar motion through the GMC.

4. The motion of an Oort-cloud comet through a GMC

In this section, we derive the equations of motion of a comet being in the OC during the passage of the solar system through the GMC with the properties more specified in the previous sections. We denote the heliocentric radius and velocity vectors of a given comet by $\boldsymbol{r}=(x,y,z)$ and $\dot{\boldsymbol{r}}=(\dot{x},\dot{y},\dot{z})$, respectively. In the mass-centre coordinate system, the radius and velocity vectors of the comet are $\boldsymbol{r}_c=(x_c,y_c,z_c)$ and $\dot{\boldsymbol{r}}_{\boldsymbol{c}}=(\dot{x}_c,\dot{y}_c,\dot{z}_c)$, respectively. The vector $\boldsymbol{r}$ is related to the vector $\boldsymbol{r}_c$ as

$$\boldsymbol{r}=\boldsymbol{r}_c-\boldsymbol{R} \qquad (25)$$

(consequently, $\ddot{\boldsymbol{r}}=\ddot{\boldsymbol{r}}_c-\ddot{\boldsymbol{R}}$).

Each condensation acts on the comet with the mass within the radius $|\boldsymbol{P}_j-\boldsymbol{r}_c|$, which is given by

$$M_{rj}=4\pi\rho_{cj}\left|\boldsymbol{P}_j-\boldsymbol{r}_c\right|^3 S_{Cj}, \qquad (26)$$

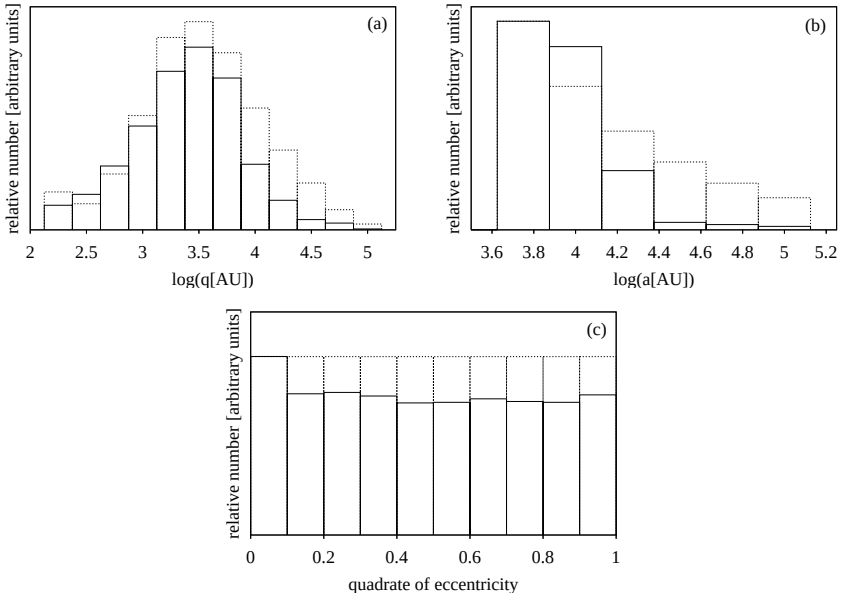

Figure 1. The distributions of the perihelion distance (a), semi-major axis (b), and square of eccentricity (c) of the comets in an outer part of the Oort cloud before (dashed-lined bars) and after (solid-line bars) a passage of the whole solar system through the hypothetical giant molecular cloud specified in Sect. 5.1.

where

$$S_{Cj} = \sum_{i=0}^{\infty} \frac{(-1)^i}{(2i+3).i!} \left(\frac{|\boldsymbol{P}_j - \boldsymbol{r}_c|}{\sqrt{2}\sigma_j} \right)^{2i} . \tag{27}$$

Having the formula for the calculation of this mass, we can construct the equations of motion of the comet. The final form of the heliocentric acceleration vector can be written as

$$\ddot{\boldsymbol{r}} = -k^2 \frac{M_\odot}{r^3} \boldsymbol{r} - 4\pi k^2 \sum_{i=1}^{j} \rho_{cj} \left[S_{Cj}(\boldsymbol{r}_c - \boldsymbol{P}_j) - S_j(\boldsymbol{R} - \boldsymbol{P_j}) \right] . \tag{28}$$

To integrate the motion of the Oort cloud through the GMC, we numerically integrate the motion of each considered theoretical comet of the comet cloud using the equations of motion (28) and, simultaneously, numerically integrate the motion of the Sun using its equations of motion (7).

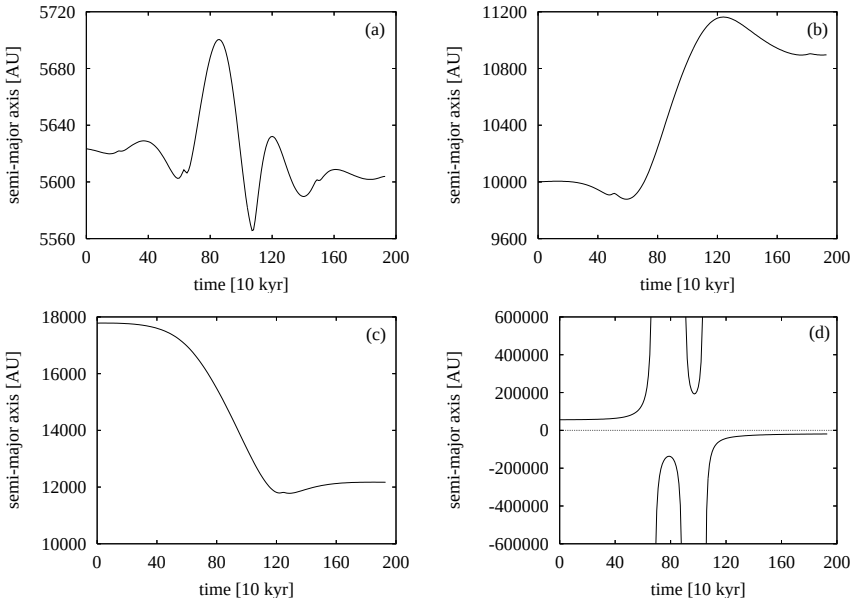

Figure 2. The examples of the behavior of the osculating semi-major axis of four OC comets, when the entire solar system passes through the theoretical GMC described in Sect. 5.1. The initial orbital elements, $log(a_o)$, e^2, ω, Ω, and $cos(i)$, of the demonstrated comets are: (a) 3.75, 0.55, 60^o, 120^o, and -0.9; (b) 4.00, 0.65, 90^o, 30^o, and -0.7; (c) 4.25, 0.65, 60^o, 30^o, and $+0.7$; (d) 4.75, 0.65, 30^o, 150^o, and $+0.7$, respectively. Notice the different vertical scale of the plots.

5. Studied examples

Let us study a few specific examples of how a theoretical GMC changes the structure of the Oort cloud when the Sun surrounded with its comet reservoir goes deeply across the GMC. Three GMCs are considered.

The initial structure of the Oort cloud is approximated by the model worked out in our earlier paper (Neslušan & Jakubík, 2005). The range of decadic logarithm of the semi-major axis is considered somewhat larger than in the previous paper: $3.75 \leq log(a_o) \leq 5.00$, since the outer part of the Oort cloud, which is only possible to be studied, can be replenished, during the passage through the GMC, from a more inner region. Because of this enlargement of the range, we reduced, on the other-hand side, the step of $log(a_o)$ to be 0.25 (a_o is given in AU). Since the other details of the model can be found in (Neslušan and Jakubík, 2005; Sect. 2.1), we only briefly summarize its basic characteristics here: the argument of perihelion, ω_o, and longitude of ascending node, Ω_o, vary from 15^o to 345^o with a step of 30^o, cosine of inclination, $cos(i_o)$, varies from

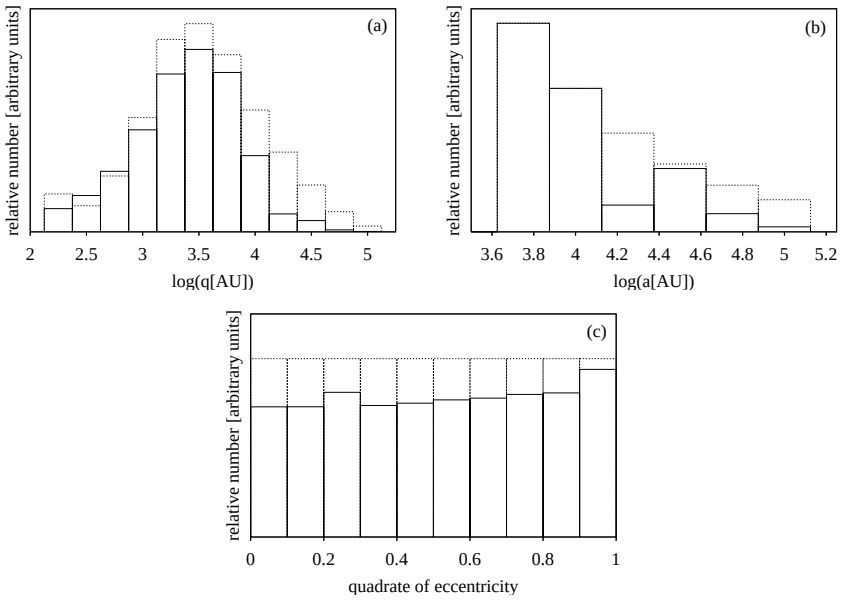

Figure 3. The distributions of the perihelion distance (a), semi-major axis (b), and square of eccentricity (c) of the comets in an outer part of the Oort cloud before (dashed-lined bars) and after (solid-line bars) a passage of the whole solar system through the hypothetical giant molecular cloud specified in Sect. 5.2.

-0.9 to $+0.9$ with a step of 0.2, and square of eccentricity, e_o^2, varies from 0.05 to 0.95 with a step of 0.1. At the beginning of the time account, each theoretical comet is assumed to be in the aphelion of its Keplerian orbit.

The model consists of orbits having all possible combinations of the above specified discrete values of the five orbital elements. It means that the model of the Oort cloud consists of 86 400 discrete orbits, in total.

We consider the same number of comets in each interval of $log(a)$, i.e. the flat distribution of semi-major axes. Since we found that the actual semi-major-axis distribution is proportional to a^{-s} with $s \approx 0.65$ (Neslušan and Jakubík, 2005), we assign to each comet a weight to fit this distribution law. The weight is assigned by the interval of $log(a)$, in which the comet's $log(a)$ is initially situated. Denoting the intervals of $log(a)$ centered at the values of 3.75, 4.00, 4.25,..., 5.00 by serial numbers $j = 1, 2, 3, ..., 6$, respectively, the weight of each comet with $log(a)$ in the j-th interval is given as

$$w_j = \frac{a_j^{-0.65}}{a_6^{-0.65}} = \left(10^{1.50-0.25j}\right)^{0.65}, \tag{29}$$

whereby $a_j = 10^{3.50+0.25j}$. Using this relation, we obtain the values of w_j equal

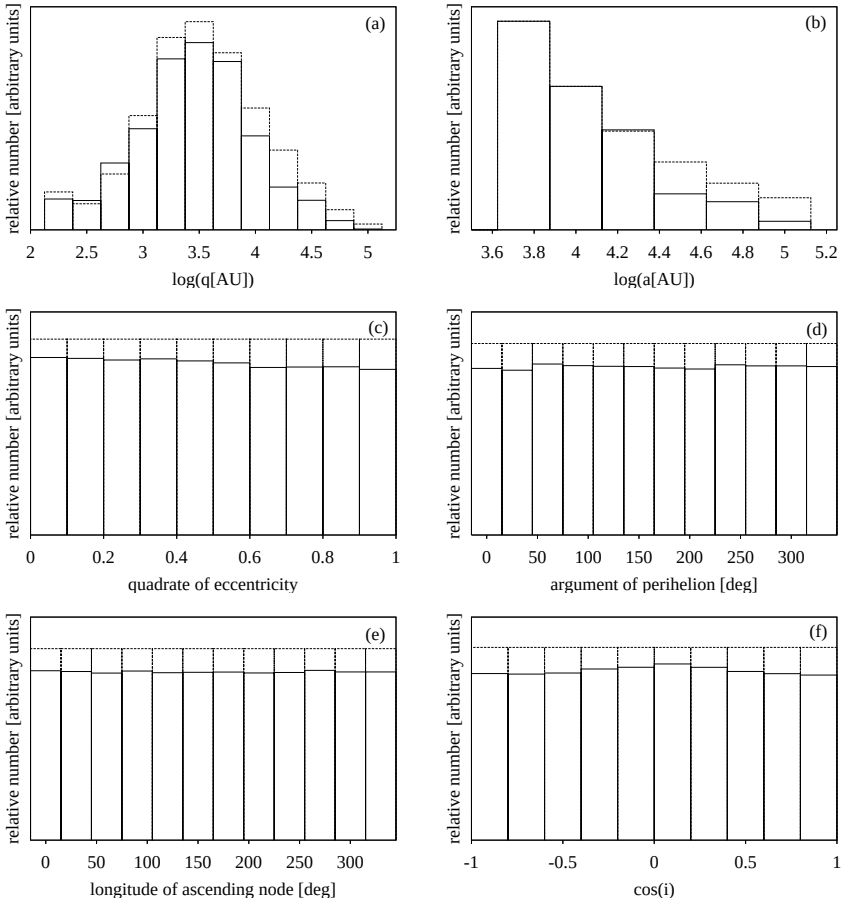

Figure 4. The distributions of the perihelion distance (a), semi-major axis (b), square of eccentricity (c), argument of perihelion (d), longitude of ascending node (e), and cosine of inclination (f) of the comets in an outer part of the Oort cloud before (dashed–lined bars) and after (solid-line bars) a passage of the whole solar system through the hypothetical giant molecular cloud specified in Sect. 5.3.

to 6.493816, 4.466836, 3.072557, 2.113489, 1.453784, and 1.000000 for $j = 1$, 2, 3, 4, 5, and 6, respectively. When the orbits are weighted, the model of the Oort cloud counts 267 846.94 orbits.

At the beginning of the numerical integration, the velocity vector of the Sun is $\dot{\boldsymbol{R}} = (-25,\ -0.5,\ -0.1)\,\mathrm{km\,s^{-1}}$.

5.1. The passage of the OC through a single-condensation GMC - I

In this case, we consider a single condensation, representing a large spherical GMC, with the mass $M_O = 1.5 \times 10^5\,\mathrm{M}_\odot$ and radius $R_O = 20\,\mathrm{pc}$. Requiring the density profile given by (2), the central density of the condensation must be $\rho_c = 8.75141 \times 10^{-18}\,\mathrm{kg\,m^{-3}}$ and dispersion $\sigma = 8.647239 \times 10^6\,\mathrm{AU}$. To describe the initial position of the Sun, we use the spherical coordinate system P, L, and B corresponding with the rectangular $u - v - w$ system. The position is characterized by $P = 1.3R_0$, $L = -3^o$, and $B = -3.5^o$. At this passage, the Sun approaches the condensation centre up to 2.22 pc.

The distributions of the perihelion distance, semi-major axis, and square of eccentricity of the OC comets after the passage through the GMC are shown in Fig. 1 (solid-line bars). For a comparison, the corresponding initial, before the passage, distributions (dashed-line bars) are shown, too. As a consequence of the passage, the OC loses 22% of its population. In Fig. 1a, we can notice a strong depletion of the outer parts of the OC: the numbers of comets with $log(a) > 4.25$ after the passage is apparently smaller than that before the passage. However, some comets are not ejected and, thus, lost, but their semi-major axes are reduced (an increase of the number for $log(a) \approx 4$).

Concerning the perihelion distance, we can see that the perihelia are enlarged in the region of $log(q) < 2.75$ (Fig. 1b). The GMC perturbing force does not, practically, influence the very low eccentric orbit, with $e^2 < 0.1$ (Fig. 1c). The distribution of the rest of e^2 range remains constant though the corresponding population decreases during the passage.

A few examples of the evolution of cometary osculating semi-major axes during the passage are shown in Fig. 2. Some semi-major axes can roughly be conserved, though otherwise they largely change, when the OC passes internal part of the GMC, as seen in plot a. Both an increase or decrease of this orbital element can occur as illustrated in plots b and c, respectively. An interesting case can be seen in plot d. At first, a strong perturbation enlarges the semi-major axis to become hyperbolic (its value is negative, formally). However, this period is short, the comet is still in the OC and perturbation acts. For another period, the semi-major axis becomes positive, the comet moves on an elliptical orbit. Finally, the comet receives another energy and, finally, becomes, second time, hyperbolic and leaves the OC.

5.2. The passage of the OC through a single-condensation GMC - II

The second model of the considered single-condensation spherical GMC has the mass $M_O = 4 \times 10^5\,\mathrm{M}_\odot$, radius $R_O = 30\,\mathrm{pc}$, central density (given by (2)) $\rho_c = 6.66915 \times 10^{-18}\,\mathrm{kg\,m^{-3}}$, and dispersion $\sigma = 1.312855 \times 10^6\,\mathrm{AU}$. The initial position of the Sun is characterized by $P = 1.3R_0$, $L = +3.5^o$, and $B = +2.5^o$. At this passage, the Sun approaches the condensation centre up to 1.79 pc.

The distributions of the perihelion distance, semi-major axis, and square of eccentricity of the OC comets after the passage are shown in Fig. 3 (solid-line bars). For a comparison, the corresponding initial distributions (dashed-line bars) are shown, again. As a consequence of the passage, the OC loses the same fraction of its population as in case I (Sect. 5.1), i.e. about 22%. This is surprising, because the mass of the condensation is 2.67 times greater than that in case I. The loss can be seen in the distribution of the semi-major axis, in plot a. A depletion occurs for $log(a) > 4.6$. An interesting feature is an almost conserved population with $log(a) \approx 4.5$, but a strongly depleted population with $log(a) \approx 4.25$. This is likely a consequence of a perturbation mechanism analogous to the resonant action in the case of the planetary perturbations. The region $log(a) < 4.1$ remains practically intact by the GMC perturbation in this case.

Similarly to case I, the perihelia are enlarged in the region of $log(q) < 2.75$ (Fig. 3b). Concerning the eccentricity, the GMC perturbing force only weakly, this time, influences highly eccentric orbits, with $e^2 > 0.9$ (Fig. 1c). The distribution of the rest of e^2 range remains roughly constant.

5.3. The passage of the OC through a two-condensation GMC

In this subsection, we investigate a consequence of the passage of OC through the GMC consisting of two condensations. Specifically, the mass and radius of the first condensation are identical to that introduced in Sect. 5.1 and the mass and radius of the second condensation are $2.5 \times 10^5\,\mathrm{M}_\odot$ and 25 pc, respectively. So, the total mass of the GMC equals the mass of the larger condensation, introduced in Sect. 5.2. The centre of the first condensation is situated at a distance of $P_1 = 26.25$ pc from the mass centre of the whole GMC (the origin of the coordinate frame used), in direction $L_1 = 105^o$, and $B_1 = +80^o$, while the centre of the second condensation is at $P_2 = 15.75$ pc, $L_2 = 285^o$, and $B_2 = -80^o$. At these values of P_1 and P_2, the separation of the condensations (the distance between their centres) is 42 pc. This distance is chosen, in purpose, to be slightly shorter than the sum of their radii. So, the condensations slightly overlap each other at their borders.

The Sun passes the mass centre of the GMC at the closest distance of 0.85 pc. After the passage, the distributions of the perihelion distance, semi-major axis, square of eccentricity, as well as angular elements, i.e. the argument of perihelion, longitude of ascending node, and cosine of inclination, of the OC comets are shown in Fig. 4 (solid-line bars). Again, the corresponding initial distributions (dashed-line bars) are also shown. As a consequence of the passage, the OC loses about 12% of its population. This is, surprisingly, less than in the case of the passages through the single-condensation GMC (Sects. 5.1 or 5.2).

The change of the perihelion-distance distribution (Fig. 4b) has a very similar character as the already described changes after the single-condensation-GMC passages. In the distribution of the square of eccentricity (Fig. 4c), no

preferred interval, when this quantity remains untouched, occurs, this time. The entire distribution remains quasi constant.

In all the studied passages, the directional distribution of orbits is almost unchanged. In Fig. 4d, e, and f, we demonstrate only the angular distributions of the OC comets in the case of the passage through the two-condensation GMC, but the corresponding distributions for the two previous passages, through the single-condensation GMCs, have practically the same, constant behavior.

6. Concluding remarks

Considering our simple models of the GMCs, with the mass comparable with an upper limit of the observed GMC masses, however, we can report only a small final effect of a passage of the solar system through a GMC on the OC. The GMC perturbation does not practically change the directional distribution of the orbits in the comet reservoir. The obvious consequence is an erosion of the outer part of this reservoir. However, even the maximal found erosion rate, when 22% of the OC population is lost, has not any fatal consequence on the comet cloud. The last studied example moreover implies that a more complicated structure of GMC may have a less erosive effect than a simple, single-spherical-condensation GMC.

After looking at many individual examples of the evolution of OC-comet-orbit semi-major axes (in the presented pictures, we showed only few illustrative examples), i.e. evolution of the orbital energy in fact, one can confirm a relatively large amplitude of many GMC perturbation effects. However, an enlarged semi-major axis is often reduced back, therefore the final effect appears to be small. Or, the effect remains large, but its result is an overall reduction of the semi-major axis.

Of course, the work described in this paper is only a small contribution to the problem. Our study goes on and we intend to assume also other, alternative models of the GMC internal structure. The results of the further study, including a much larger variety of the encounter geometry, will be presented in future papers.

Acknowledgements. The authors thank the project "Enabling Grids for E-sciencE II" for the provided computational capacity. They also acknowledge the partial support of this work by VEGA − the Slovak Grant Agency for Science (grant No. 7047).

References

Bailey, M.E.: 1986, *Mon. Not. R. Astron. Soc.* **218**, 1

Biermann, L.: 1978, *Astron. Papers Dedicated to Bengt Strömgren, Symposium*, Copenhagen, 327

Clube, S.V.M., Napier, W.M.: 1984, *Mon. Not. R. Astron. Soc.* **208**, 575

Hut, P., Tremaine, S.: 1985, *Astron. J.* **90**, 1548

Mazeeva, O.A.: 2004, *Solar System Res.* **38**, 325
Napier, W.M., Staniucha, M.: 1982, *Mon. Not. R. Astron. Soc.* **198**, 723
Neslušan, L., Jakubík, M.: 2005, *Astron. Astrophys.* **437**, 1093
Solomon, P.M., Rivolo, A.R., Barrett, J., Yahil, A.: 1987, *Astrophys. J.* **319**, 730